






A computational approach for Leishmania

genus protozoa detection in bone marrow samples from patients with visceral Leishmaniasis

Un enfoque computacional para la detección de protozoos del género Leishmania en muestras de médula ósea de pacientes con leishmaniasis visceral

 Angélica Isaza-Jaimes¹,  Valmore Bermúdez²,  Antonio Bravo³,  Jhoalmis Sierra Castrillo⁴,  Juan Diego Hernández Lalinde⁵,  Cleiver A Fossi¹,  Anderson Flórez¹,  Johel E Rodríguez¹

¹Universidad Simón Bolívar, Facultad de Ingenierías, Cúcuta, Colombia.

²Universidad Simón Bolívar, Facultad de Ciencias de la Salud, Barranquilla, Colombia.

³Programa Calidad y Productividad Organizacional, Decanato de Investigación, Universidad Nacional Experimental del Táchira, San Cristóbal 5001, Venezuela.

⁴Universidad de Santander, Grupo de Investigación BIOGEN, Departamento de Salud, Cúcuta.

⁵Universidad Simón Bolívar, Departamento de Ciencias Sociales y Humanas, Cúcuta, Colombia.

Corresponding author: Johel E Rodríguez, Universidad Simón Bolívar Sede Cúcuta, Avenida 4 con Calle 14, Bloque G, Barrio La Playa, Cúcuta, Norte de Santander, Colombia, e-mail: jrodriguez116@unisimonbolivar.edu.co

Received/Recibido: 08/28/2020 Accepted/Aceptado: 09/15/2020 Published/Publicado: 11/09/2020 DOI: 10.5281/zenodo.4426403

Abstract

This article reports a three-stage computational approach for the automatic detection of *Leishmania* protozoan in light microphotograph from bone marrow samples extracted from patients with visceral Leishmaniasis. The first stage corresponds to the pre-processing of the microscopy images, in which initially a low-pass filter or softener was applied to attenuate the undesired information associated with the images and preserve the edges in the objects contained in the images. The pre-processing stage concluded with the application of consistent gradient operators to the smoothed images to emphasise the changes of the intensities associated with the protozoa edges by determining the gradient module. In the second stage, a procedure-oriented to the selection of regions of interest that were candidates to contain parasites in the pre-processed images was developed, based on the intensity analysis associated with a set of intensity profiles selected from the smoothed images. In the final stage, each region of interest containing protozoa was analysed on the gradient module by a technique based on polar maps, to classify its content as a parasite of the genus *Leishmania* or not. The application of the proposed computational approach to a set of samples of patients with Visceral Leishmaniasis generated a recognition parasite percentage of approximately 80%.

Keywords: Protozoan, *Leishmania*, micrographics, anisotropic diffusion, gradient operator, intensity profiles.

Resumen

Este artículo reporta un enfoque computacional en tres etapas para la detección automática de protozoos del género *Leishmania* en microfotografías a partir de muestras de médula ósea extraídas de pacientes con Leishmaniasis visceral. La primera etapa correspondió al preprocesamiento de las imágenes de microscopía, en la que inicialmente se aplicó un filtro de paso bajo para atenuar la información no deseada asociada a las imágenes y preservar los bordes en los objetos. La etapa de preprocesamiento concluyó con la aplicación de operadores de gradiente a las imágenes suavizadas para enfatizar los cambios de las intensidades asociadas con los bordes de los protozoos. En la segunda etapa se elaboró un procedimiento orientado a la selección de las regiones de interés candidatas a contener parásitos, sobre la base del análisis de intensidad asociado a un conjunto de perfiles seleccionados a partir de las imágenes suavizadas. En la etapa final, cada región de interés que contenía protozoos fue analizada en el módulo de gradiente mediante una técnica basada en mapas polares de forma de clasificar su contenido como parásito del género *Leishmania*. La aplicación del enfoque computacional propuesto generó un porcentaje de reconocimiento del parásito de aproximadamente el 80%.

Palabras clave: Protozoario, *Leishmania*, micrografía, difusión anisotrópica, operador de gradiente, perfiles de intensidad.

Introduction

Leishmaniasis is a disease caused by an obligate intracellular protozoan from the genus *Leishmania* and transmitted by the sting of an infected *Phlebotomus* or *Lutzomyia* genus flying arthropods¹, presenting three different clinical forms: a) visceral leishmaniasis (VL), b) cutaneous leishmaniasis (CT),

and, c) mucocutaneous Leishmaniasis (MCL). Leishmaniasis is one of the most crucial vector-transmitted diseases in the world. In fact, according to the World Health Organization (WHO), an estimated 12 million cases of Leishmaniasis worldwide with an annual incidence of both, 500,000 and

1,500,000 new cases of VL and CL, respectively. Leishmania infection has a worldwide distribution, being endemic in tropical and subtropical regions of 88 countries. There are an estimated 12 million cases in the Americas, the Mediterranean region and western Asia²⁻⁵.

The majority of CL cases occur in Afghanistan, Algeria, Brazil, Colombia, Iran, Pakistan, Peru, Saudi Arabia and Syria. In 2017, 20.792 new cases reported was diagnosed in seven countries: Brazil, Ethiopia, India, Kenya, Somalia, South Sudan and Sudan. In this context, Colombia had one of the highest numbers of Leishmania species affecting humans in the world exhibiting nine species of these genus parasites [6]. Most cases are CL, and a small proportion is represented by MCL and VL cases. Currently, 449-second sub-national administrative levels (Municipalities) are endemic for CL with 20 million inhabitants at risk. Between 2000 and 2016, about 177,468 CL cases were reported, peaking at 18,043 in 2005. Since then, at least 10,000 cases have been reported annually⁷.

Historically, leishmaniasis diagnosis has been confirmed by isolating, visualising, and culturing the parasite from infected tissue. CL confirmation implies performing tissue biopsies, dermal scrapings, and needle aspirates. The sample is usually stained in Leishman, Giemsa, or Wright stains and then examined under the microscope. For VL, the parasite can be observed through direct tissue-resident amastigotes visualisation, from peripheral blood, bone marrow, liver, or spleen aspirates. In both the CL and MCL, cell-mediated immunity against the parasite is very strong, and the density of this parasite in the skin/mucosa is low, i.e. in the case of long-standing disease. Despite this, microscopy with Giemsa stains can reveal the protozoa in up to 80% of cutaneous leishmaniasis specimens. Usually, *Leishmania donovani* is best detected by doing a thick film and creating a single straight leukocyte edge when making a peripheral smear or by centrifugation of citrated blood and withdrawing the sediment, which is then smeared, dried, and stained⁸.

In the other hand, immunodiagnostic tests have used for diagnosis of VL Leishmaniasis, especially, the indirect fluorescent antibody (IFA) technique, which is 80-100% sensitive in patients with VL mainly in patients not infected with human immunodeficiency virus. The development of PCR has provided a powerful approach to the diagnosis of Leishmaniasis. Primers designed to amplify conserved sequences of minicircle kinetoplast DNA found in Leishmania parasites have been described with much better sensitivity (92-99%) and specificity (100%) in comparison with other methods, especially in recent-onset disease. Unfortunately, the best diagnostic tests are not frequently available in endemic and emerging countries. Therefore Leishmaniasis diagnosis is often made by both, epidemiological data and physical examination and direct microscopy methods⁹⁻¹¹.

The direct analysis of both microorganisms is cheaper than PCR or IFA. However, it requires a microbiology specialist and a considerable time expenditure process analysing each image and then, the repetition of this process several times on other images of the same patient. Therefore, the

process is slow, time-consuming, and associated with errors attributable to tiredness due to the repeated observations necessary to analyse the samples. However, technological advances in high-speed mobile phone-based internet, android applications, smartphone high-end photographic cameras, cell-phone-couple microscope, 3D printer technology and, a pleiad of advances in methods for automatic images analysis and artificial intelligence approach have opened a new horizon in the diagnosis of some infectious diseases¹². Thus, soon, the next solution will be in a smartphone camera equipped with a 3D printed magnifying device armoured with both an artificial intelligence chip and an image recognition software capable of identifying Leishmania parasites automatically. Moreover, now Android-based phones are inexpensive, even in poor-resource settings like ours.

In this vein, it is essential for developing countries to improve the diagnosis of Leishmaniasis and other protozoa diseases, maintaining a good cost-effectiveness profile, improving the specificity and sensitivity, and making a quick diagnosis on a large number of histological samples from the same patient. In this sense, this article proposes a new computational approach for automatic detection of protozoa parasites from *Leishmania* genus from microscope images of VL.

Method

Methodology

The purpose of the research was to develop a useful computational approach for the automatic detection of protozoa parasites, causing visceral Leishmaniasis. The present study considers 45 images that have been acquired from samples of patients with visceral Leishmaniasis by light-microscope¹⁵. This images set can be found at <https://sites.google.com/site/hosseinrabbanikhorasgani/datasets-1/dataset-of-leishmania-parasite-in-microscopic-images> an open dataset for clinical and computation research. It is important to note that data acquisition was made with a digital camera (Sony DSC-H9) coupled on an optical microscope (Olympus-CH40RF200) was used. The spatial resolution of the images is 3840 × 2880 pixels with a 24-bit RGB colour pixel size.

Development Phases

According to the nature of the research, the proposed computational approach is developed under a software engineering process model¹⁶, which considers the methods, tools to use, controls and outputs that are required. In this sense, it is proposed that the computational approach is supported in three stages of development. Initially, a pre-processing stage of microscopy images is required to balance the intensity levels of the pixels corresponding to the background of the images and highlighting the parasites that are very faint or little differentiated. In a second stage, a set of regions of interest in the pre-processed images are selected, to identify regions of the candidate images to contain parasites. Finally, the candidate regions of interest are analysed to determine whether or not they contain parasites of the Leishmania genus.

Image's adequation procedures

Images acquired directly from the microscope correspond to RGB colour images. However, they are converted to gray-scale images (i_{gray}) through the weighted sum of their three RGB components (i_R, i_G, i_B), according to Equation 1¹⁷.

$$i_{gray}(i, j) = 0.299 * i_R(i, j) + 0.587 * i_G(i, j) + 0.114 * i_B(i, j) \quad (1)$$

In which $0 \leq i \leq 2880$ and .

Also, as stated in its webpage, the images were previously analysed by microbiologist regarding both parasites presence and localisation.

Processing phase

The application of two types of filters is considered; an image enhancement filter or softener filter or low pass filter, based on anisotropic diffusion, and an edge enhancement filter based on the gradient module.

Anisotropic diffusion Filter

The anisotropic diffusion filter was formulated for noise attenuation or unwanted information while preserving specific features of the processed images¹⁸. The objective of this filter is to differentiate the parasites information from the background image. The standard isotropic diffusion filters such as the Gaussian filter are used to give a blur to the edges between objects of interest and the background, which makes the original position of the edges vary once the image is processed¹⁹. Nevertheless, the anisotropic diffusion filters are formulated for the edges preservation in the objects contained in the filtered images. In some cases, the anisotropic diffusion filters can be used as multiresolution descriptions of the processed images²⁰. The method is based on transforming the image as a function of its derivatives in a greater dimension space, this transformation in the space of greater dimension represented the solution of the heat equation (equation 2).

$$\frac{dI(x, y; t)}{dt} = \nabla c(x, y) \nabla I(x, y; t) \quad (2)$$

in which $I(x, y; 0)$ represents the original image, $(x, y) \in R$, t is equal to the time, and c is the conductance as a function (x, y) .

In this investigation, the anisotropic diffusion filter is computationally implanted using the class `VtkImageAnisotropicDiffusion2D` of the class library of various image processing techniques Toolkit (VTK)²¹.

Gradient module

The gradient module is used as an edge enhancement technique to improve the information associated with the contours of the parasites present in the microscopy images processed with the anisotropic diffusion filter. The operators used to obtain the directional gradients in x and y from the filtered images are constructed using the consistency criterion proposed by Ando²². The optimal 5×5 ($\nabla_{5 \times 5}$) operations presented

in [22, p. 258] used to obtain the directional gradients from which the gradient module is calculated.

Selection of interest regions

Profile selection

The proposed computational approach considers the analysis of some areas of the images instead of their exhaustive analysis since the computational cost that represents any type of analysis on the whole image is high due to its size. To this end, it is proposed to analyse a series of profiles selected and extracted dynamically from each image processed with the anisotropic diffusion filter. Each profile represents a set of image intensities associated with pixels located along a segment of the horizontal line whose size is the width of the filtered image. Each profile is regularly spaced on the top of the image. The spacing size between each profile is established *a priori* from the clinical expert who documented the samples analysed in the microscope. It is considered that the profiles should be equally spaced no more than 2×10^{-3} mm (2 μ m).

Selection of interest regions

For each profile selected, the mean quadratic deviation is determined. This statistic represents the dispersion of the intensities of the profile (ip) with respect to its mean value (Equation 3),

$$\underline{desv}^2 = \frac{1}{n} \sum_{i=1}^n |ip(i) - \underline{ip}|^2 \quad (3)$$

in which \underline{ip} is the intensities' average of the profile and n the size of the profile.

The mean quadratic deviation is considered a threshold value used to define the pixel over the profile in which a border of a parasite-candidate object is verified. Due to the ellipsoidal parasites form at the microscope, each candidate can be defined by two edges on the profile. The first edge of a parasite candidate is verified if the intensity of the filtered image goes from higher to lower than that threshold. In contrast, the second edge is identified on the pixel with an intensity exceeding the preset threshold according to the median quadratic deviation. All parasites identified by the two edges positions was labelled on the images with a square whose centre is the median defined from the positions of both edges, and with a size of 8 μ m. These labels represent the regions of interest to be analysed later.

Analysis of the interest regions

The m regions of interest located with the method described in the previous section correspond with m regions, on each microscope image, which are candidates to contain a protozoa parasite causing visceral Leishmaniasis. The information contained in each region of interest was analysed with the objective of checking whether it is associated with a parasite or not. In this sense, the information in each region of the anisotropic diffusion filter enhanced-image and the information in the image representing the gradient module were analysed.

Each region of interest extracted from the enhanced image is processed using a Gaussian density function²³ to smooth (incorporating blur) the edges strongly preserved by the anisotropic diffusion filter. The density function is defined with a

deviation standard (σ) that is equal to the deviation standard of the region located on the enhanced image with the anisotropic diffusion filter. The grey value of the central pixel in the softened region with the Gaussian density function is compared to all pixels belonging to the borders of that region.

These new candidate regions were analysed with a bimodal histogram verification algorithm²⁴, which is responsible for confirming whether the region of interest is formed by both an object and its corresponding background. All strong candidates regions to containing parasites detected are located in the image of the gradient module in order to recognise whether or not they contain a parasite. The idea is to construct a polar map of the pixel intensities associated with profiles mapped from the central pixel of the region of interest in the gradient module image to the edge of such a region. The polar map of the profile intensity is defined as the intensity variation of samples concerning the relative direction in polar coordinates²⁵.

Since the shape of the protozoa parasites of the *Leishmania* genus is approximately ellipsoidal, the polar map should show five inflexion points, two maximums and three minimums or three maximums and two minimums. Those regions of interest on the image of the gradient module whose polar map verify the five inflexion points are recognised as parasites.

Results

Data analysis techniques

Each image from the original data set was initially converted from RGB to grayscale images using the equation described in (1). **Figure 1** shows both, the original images without transformation (a, b and c) and the grayscale transformed images (d, e and f), then, they were first processed by anisotropic diffusion filters and later by a gradient module. Figure 2 shows the results obtained when applying such filters; the first row displays the result of applying the anisotropic diffusion filter, while the second row shows the gradient module.

Figure 1. Light-microscopy conventional images from patients with visceral Leishmaniasis showing contrast features. (a) High-contrast image (b) Image with contrast problems. (c) Low-contrast image; Images of patients with visceral Leishmaniasis. (d) High contrast image. (e) Image with problems in contrast. (f) Low-contrast image.

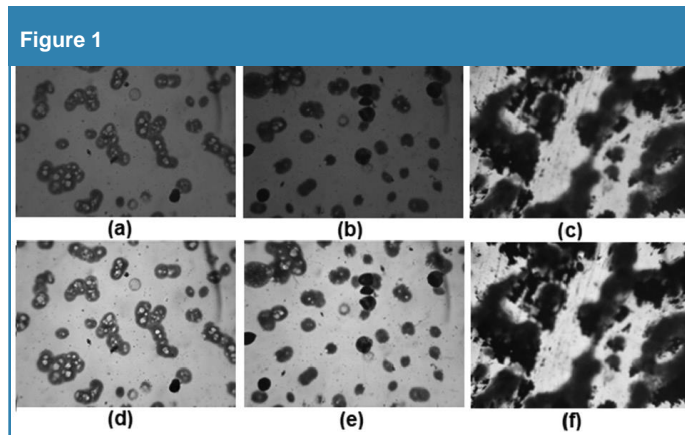


Figure 2. Pre-processed sample images from patients with visceral Leishmaniasis. (a) High-contrast image. (b) Image with contrast problems. (c) Low-contrast image.

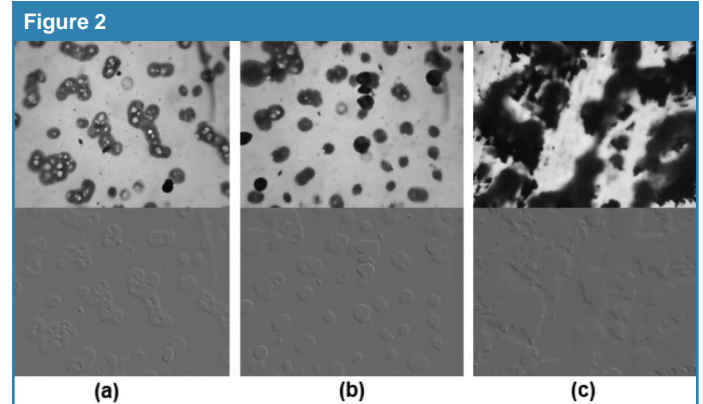
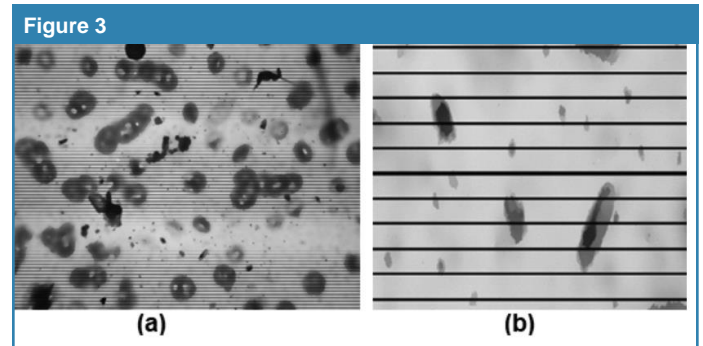


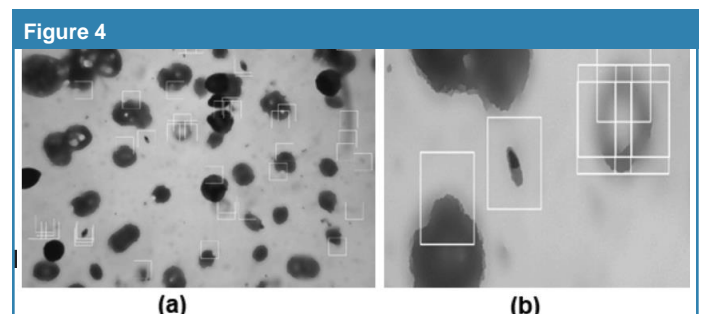
Figure 3 exhibit the selected profiles on an image with parasites of the *Leishmania* genus processed with the anisotropic diffusion filter. The profiles are plotted according to horizontal lines of 3840 pixels separated every thirty (30) pixels in a vertical direction. A total of 128 profiles are plotted on each microscope image Figure 3(a). Figure 3(b) shows a particular region of the image (rescaled in size), in which it is verified that the profiles cut-off some parasites.

Figure 3. Image filtered by anisotropic diffusion filter with the selected profiles. (a) Mapped profiles. (b) Region of the rescaled image in dimension



The analysis of the profiles through the criterion based on the median quadratic deviation generates the first set of candidate regions to contain parasites within the microscope sample images of patients with protozoa of the *Leishmania* genus. Figure 4 shows an image with all regions estimated by the profile analysis method.

Figure 4. Image filtered by anisotropic diffusion filter with the selected regions. (a) Selected regions. (b) Region of the rescaled image in dimension.



For each selected region is applied the analysis scheme of interest regions described in section 2.4, with the help of the profile analysis procedure based on the mean quadratic deviation. This scheme allows recognising the regions containing the parasites of the *Leishmania* genus. Figure 5 shows the parasites recognised by the computational approach and the parasites documented by an expert on a microscopy image.

Figure 5. Results obtained on a microscope image. (a) Results after applying the proposed approach in this paper, parasites are labelled in green. (b) Parasites are documented by a specialist, parasites are labelled in red.

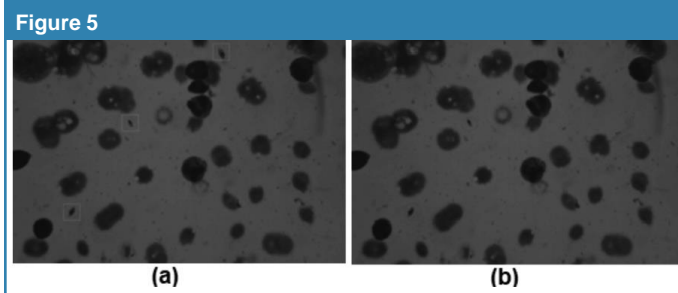


Table 1 shows the results obtained on all 45 images of patients with parasites of the *Leishmania* genus processed.

Table 1. Number of parasites recognised for each processed image

Image	Quantity of parasites		Image	Quantity of parasites		Image	Quantity of parasites	
	Labelled	Recognised		Labelled	Recognised		Labelled	Recognised
1	3	3	16	2	1	31	3	2
2	2	1	17	2	1	32	6	5
3	1	1	18	2	2	33	3	2
4	1	1	19	1	1	34	1	1
5	1	1	20	1	0	35	6	6
6	1	1	21	1	1*	36	2	1
7	1	1	22	2	2	37	1	1
8	1	1	23	1	1	38	2	2
9	6	4	24	1	1	39	2	1
10	1	1	25	1	1	40	6	6
11	2	1	26	1	1	41	5	4
12	2	1	27	3	3	42	5	3
13	2	1	28	1	1	43	1	1
14	2	1	29	2	2	44	2	2
15	2	1	30	4	3	45	1	1

* This value corresponds to a false positive

Technical implementation and execution time

A desktop computer with an Intel (R) Core (TM) i7-6500 CPU (@ 2.50 GHz 2.59 GHz), 12 GB RAM, and Linux operating system 64 bits was used to run the computational approach.

The computational approach is encoded using C++ and VTK. As for VTK, the reading and writing classes files in JPG format was used, specifically VtkJPEGReader and vtkJPEGWriter whose input parameters correspond to the names of the images to read or write. Additionally, the VtkImageAnisotropicDiffusion2D class was used to implant the anisotropic diffusion filter, class that requires as input parameters the conductance or diffusion parameter (c), which was set to C=3, the number of iterations that it concerns the largest dimension space considered by the filter and was set at 250. It also receives as input parameter the threshold used as a diffusion stop criterion, which was set to 5. All other classes or functions that support the computational approach was coded using C++.

The application of the pre-processed filters requires 26.5 s of runtime. The execution time of the selection procedures and analysis of the profiles is of approximately 0.37 s; while the final recognition of the protozoa requires 0.24 s of runtime. The total execution time of the computational approach proposed by each image of patients with visceral Leishmaniasis is 27.11 s.

Discussion

Intracellular protozoan parasites are responsible for worldwide infectious diseases with a high impact in public health for developing countries. Among them, *Leishmania* parasites are causative agents of Leishmaniasis, a worldwide endemic disease with a variety of parasite species, reservoirs and vectors involved in their transmission with diverse clinical manifestations ranging from self-healing skin ulcers to life-threatening visceral disease with a fatal outcome in 7% of the infected patients. In this regard, *Leishmania* genus comprises about 22 pathogenic species to humans. In the Americas, human infection occurs by 15 species, which are grouped in the *Leishmania* and *Viannia* subgenera. In our region, the three most important species of *Leishmania* subgenus are *L. mexicana*, *L. amazonensis* and *L. venezuelensis*. These species are morphologically indistinguishable but can be differentiated by analysis of isoenzymes, molecular methods or monoclonal antibodies.

In general terms, Leishmaniasis affects mainly the most impoverished populations, as it is associated with poor housing conditions and lack of economic resources; Besides, it is linked to environmental changes such as deforestation and urbanisation, including movements of the population due to conflicts and drug trafficking, as well as significant risk factors 4,7,8. By now, the geographic distribution of the disease

is limited to areas where vectors are capable of spreading, added to the physiological and biological profile of the infecting species 4,5. Thus, the epidemiology of CL in the Americas is complex, with a wide variation in transmission cycles, reservoir hosts, sandfly vectors, clinical manifestations and response to therapy, and the interaction of multiple Leishmania species in the same geographical area^{6-7,10,26-28}. By all these reasons, Leishmaniasis is one of the most critical vector-transmitted disease in the world and an intensive matter of study. Nonetheless, despite the abundant number of studies on Leishmaniasis, classically, investigations have focused on Epidemiological, clinical, and preclinical aspects regarding the burden of the disease. At the same time, research related to new alternatives in diagnostic aids, i.e. new diagnostic tools like smartphone microscopy or automated parasite identification is meagre for this disease. On the other hand, from an economic perspective, health faces challenges, especially in endemic countries for Leishmaniasis in which a restrictive economy predominates, with wide gaps between health needs and the organisational capacity in the health system, shows the need to rationalise spending, maximise benefits and the general increase the efficiency in the allocation of health resources. In this sense, access to rapid and reliable diagnosis in poorly-health served remote rural areas and even in deprived urban settings lack adequate health services is imperative in order to minimise the human and economic impact of this condition²⁹⁻³⁰.

In this framework of technological advances, the refinements in precision optic lenses in high-end mobile phones photographic cameras and the advances in automatic images analysis and artificial intelligence show a shift in new diagnostic approach affordable to countries with scarce financial resources. For example, in a recent study conducted by Coulibaly et al. in³¹ Côte d'Ivoire a handheld diagnostic devices (Newton Nm 1microscope and a clip-on version of the mobile phone-based CellScope) were used for the diagnosis of *Schistosoma haematobium*, *S. mansoni*, and intestinal protozoa infection in a community-based survey. The accuracy of these devices was compared to conventional light microscopy showing a prevalence of *S. haematobium*, *S. mansoni*, *G. intestinalis*, and *E. histolytica/E. dispar*, as determined, was 39.8%, 5.3%, 20.7% 4.9%, respectively (Conventional microscopy). The Newton Nm1 microscope had diagnostic sensitivities for *S. mansoni* and *S. haematobium* infection of 91.7% and 81.1%, respectively, and specificities of 99.5% and 97.1%, respectively. The CellScope demonstrated sensitivities for *S. mansoni* and *S. haematobium* of 50.0% and 35.6%, respectively, and specificities of 99.5% and 100%. For *G. intestinalis* and *E. histolytica/E. dispar*, the Newton Nm1 microscope had a sensitivity of 84.0% and 83.3%, respectively, and 100% specificity. All of these diagnostic procedures were made by trained laboratory technicians³¹. This investigation and others have demonstrated the feasibility of microbiological diagnosis of this type of hardware, bringing to us the necessity of algorithms oriented to pathogens recognition.

In this regard, most research in this area has been oriented to recognise the most killing parasite infection, Malaria. The

prospects of automating malaria diagnosis with its apparent advantages have attracted many researchers, especially in the last decade, and result obviously that all knowledge in pattern recognition of *Plasmodium* can be translated to Leishmania research. For example, Dallet et al. described a mobile application platform for Android phones that can diagnose malaria from Giemsa-stained thin blood film images³². The application was based on a novel Annular Ring Ratio Method which is already implemented, tested and validated in MAT-LAB. The method detects the blood components such as the Red Blood Cells, White Blood Cells, and identifies the parasites in the infected RBCs. The application also recognises the different life stages of the parasites and calculates the parasitemia, which is a measure of the extent of infection. The application takes less than 60 seconds to give a diagnosis and has been tested and verified on several version and types of Android mobile phones and tablets.

In the same context, Saeed et al.³⁰, have developed a smartphone application to compute parasitemia in Giemsa-stained thin blood film images. In order to segment individual red blood cells, they applied Marker-Controlled Watershed MC-W to thin blood smears to efficiently detect and segment individual cells, separate touching cells, and meet the demand of real-time processing. In the cell detection step, a multi-scale Laplacian of Gaussian (LoG) filter on the green channel of an RGB colour slide image was applied. The local extrema of the LoG response indicate the approximate centroids of the individual cells that will serve as the approximate centroids for the MC-W segmentation step.

Rosado et al.³³, presented an image processing and analysis methodology using supervised classification to assess the presence of *P.falciparum* trophozoites and white blood cells in Giemsa stained thick blood smears. Using a support vector machine (SVM) and a mix of geometric, colour, and texture features, their automatic detection of trophozoites achieved a sensitivity of 80.5% and a specificity of 93.8%, while their white blood cell detection achieved 98.2% sensitivity and 72.1% specificity.

Very few studies have automatic study detection of Leishmania protozoa in tissues sample with an affordable approach. Farahi et al.³⁴, the author of the Leishmania database used in this work, achieved the segmentation of Leishmania from bone marrow smear with Giemsa-stained images. In the Farahi's approach, linear contrast stretching method follows by the morphological method was used to extract suspicious samples with Leishmania. Then, a morphological method was used in order to segment the nuclei in each extracted sub-images separately. Additionally, the level set method was employed to elicit the precise boundary of parasite's cytoplasm. In addition to the global model, a local model was proposed to hasten the algorithm. Obtained percentage of the mean of segmentation error is 10.90% for global model and 9.76% for the local model. The authors hypothesise that any desired features could be extracted in order to detect the Leishmania parasites.

According to the information shown in table 1, the recognition percentage achieved by our proposed computational ap-

proach is 78.79%, with a false positive. On 61.37% of the images, the parasites' recognition was reached in 100%, whereas in 38.64% of the samples, the recognition was between 50% and 80%. In absolute values, of the 99 parasites that are identified or documented by an expert in the 45 samples analysed, the proposed computational approach allows recognising 78 of protozoa parasites of the Leishmania genus present in the microscopy images of such samples. The filtering technique based on the anisotropic diffusion filter allows correcting the inhomogeneity background of the images associated with the pigmentation process of the analysed samples. Meanwhile, the consistent gradient operators used to determine the gradient module allows emphasising the intensity changes associated with the protozoa edges. Likewise, analysis and selection of the interest regions on the intensity profiles procedures, and for the depuration of the interest regions in which the presence of parasites is estimated allow discriminating if the information belongs or not to a protozoan.

In the execution tests of the computational approach that were carried out using different sample images of Visceral Leishmaniasis and considering 128 profiles of intensities, was obtained that the recognition percentage in these tests was high, with about 80% of detection. However, the error recognition percentage reaches 21.21%, indicating that more than one-fifth of the parasites documented by the specialist had not been correctly recognised. The runtime of the computational approach is not high, the stage that consumes the most time to run is the pre-processing, and the application requires approximately 99% of this time for the anisotropic diffusion filter.

Research in microscopy imaging produces large amounts of data, which requires anywhere from full days to weeks to classify and annotate. In a single laboratory, the number of images can quickly ascend to thousands with merely one hundred patients. Not only does this detract the researchers from exploring new alternatives, as it also introduces inter-person variance, as many images are extremely cluttered and contain several hundreds of cells and parasites. These results are a time-consuming and mentally straining process, which expresses itself as a decaying function over time as the subject gets tired, frustrated or bored. These reasons justify the need for the development of automatic mechanisms able to aid researchers in repetitive daily task, for which and to the best of our knowledge, no current solution exists. The proposed method provides a fully automatic, real-time pipeline for the identification of infected cells by Leishmania using light microscopy imaging technique.

References

1. Killick-Kendrick, R., Phlebotomine vectors of the leishmaniasis: A review. *Medical and Veterinary Entomology*, 4(1):1-24, 1990.
2. Gradoni L. A Brief Introduction to Leishmaniasis Epidemiology. In: *The Leishmaniasis: Old Neglected Tropical Diseases* [Internet]. Cham: Springer International Publishing; 2018 [cited 2019 Apr 28]. p. 1–13. Available from: http://link.springer.com/10.1007/978-3-319-72386-0_1
3. Salgado-Almarío J, Hernández CA, Ovalle CE. Distribución geográfica de las especies de Leishmania en Colombia, 1985-2017. *Bio-médica* [Internet]. 2019 [cited 2019 Apr 28];39(Sp.2):1–10. Available from: <https://www.revistabiomedica.org/index.php/biomedica/article/view/4312>
4. Makerere Medical School. A, Yinusa W, Giwa S. African health sciences. [Internet]. Vol. 11, African Health Sciences. Faculty of Medicine, Makerere University; 2001 [cited 2019 Apr 28].1329–1337 p. Available from: <https://www.ajol.info/index.php/ahs/article/view/185594>
5. Cardona Arias JA, Patiño-Martínez DA, López Carvajal L. Evaluaciones económicas en Leishmaniasis cutánea: revisión sistemática de literatura 1980-2014. *Rev Econ del Caribe* [Internet]. 2017 [cited 2019 Apr 21];2(20):52–70. Available from: http://rcientificas.uninorte.edu.co/index.php/economia/article/view/8580/html_398
6. WHO | Epidemiological situation. WHO [Internet]. 2018 [cited 2019 Apr 28]; Available from: <https://www.who.int/leishmaniasis/burden/en/>.
7. World Health Organization. Disease distribution of new VL and CL cases at municipality level per 10,000 population (2015) Cutaneous Leishmaniasis, Colombia. [Internet]. 2017 [cited 2019 Apr 21]. Available from: www.who.int/leishmaniasis/Map-VL-Colombia-2015.png
8. Stark CG, Vidyashankar C. Leishmaniasis [Internet]. Medscape. [cited 2019 Apr 28]. p. 1–8. Available from: <https://emedicine.medscape.com/article/220298-workup>
9. Sundar S, Rai M. Laboratory Diagnosis of Visceral Leishmaniasis. *Clin Diagn Lab Immunol* [Internet]. 2002 [cited 2019 Apr 21];9(5):951–8. Available from: <https://www.ncbi.nlm.nih.gov/pmc/articles/PMC120052/pdf/0013.pdf>
10. Manual de procedimientos para la vigilancia y control de las leishmaniasis [Internet]. [cited 2019 Apr 21]. Available from: www.paho.org
11. González-Marcano E, Kato H, Concepción JL, Márquez ME, Mondolfi AP. Polymerase Chain Reaction Diagnosis of Leishmaniasis: A Species-Specific Approach. In: *Methods in molecular biology* (Clifton, NJ) [Internet]. 2016 [cited 2019 Apr 21]. p. 113–24. Available from: <http://www.ncbi.nlm.nih.gov/pubmed/26843051>
12. Paul Bird, Imaging in the Mobile Domain, *Rheumatic Disease Clinics of North America*, Volume 45, Issue 2, 2019, [cited 2019 Apr 21], Pages 291-302, ISBN 9780323678629, <https://doi.org/10.1016/j.rdc.2019.01.002>
13. Namakforoosh, M., Metodología de la investigación. Editorial Limusa, México, 2000.
14. Cegarra, J., Metodología de la investigación científica y tecnológica. Ediciones Díaz de Santos, España, 2011.
15. M. Farahi, H. Rabbani, A. Mehri, "Automatic Boundary Extraction of Leishman Bodies in Bone Marrow Samples from Patients with Visceral Leishmaniasis", *Journal of Isfahan Medical School*, vol. 32, no. 286, 3rd week, July 2014. Dataset: <https://sites.google.com/site/hosseinarabbanihorasgani/datasets-1/dataset-of-leishmania-parasite-in-microscopic-images>
16. Pressman, R., Ingeniería de software un enfoque práctico. McGraw Hill, España 2005.
17. Hunt, R.W.: The Reproduction of Colour, Series in Imaging Science and Technology, 6ta edición, John Wiley & Sons, 2005
18. Cañero, C., Radeva, P.: Vesselness enhancement diffusion. *Pattern*

Recognition Letters 24(16): 3141–3151, 2003.

19. Meijering, H.: Image Enhancement in Digital X-Ray Angiography. Tesis de Doctorado, Utrecht University, 2000.
20. Frangi, A., Niessen, W., Vincken, K., Viergever, M.: Multi-scale vessel enhancement filtering. In: Proceedings International Conference on Medical Image Computing and Computer Assisted Intervention. Lecture Notes in Computer Science, Germany, 130–137, 1998.
21. Schroeder, W. The Visualization Toolkit: an object-oriented approach to 3D graphics. Kitware, Clifton Park, N.Y, 2006.
22. Ando, S. Consistent gradient operators. IEEE Transaction on Pattern Analysis and Machine Intelligence, 22(3):252–264, 2000.
23. Pauwels, E., Frederix, G. Finding salient regions in images: Non-parametric clustering for images segmentation and grouping. Computer Vision and Image Understanding 75(1-2):73-85, 1999.
24. Liu, Y. Study on Automatic Threshold Selection Algorithm of Sensor Images, Physics Procedia, 25:1769-1775, 2012.
25. Qian, X., Brennan, M., Dione D., Dobrucki, W., Jackowski, M., Breuer, C., Sinusas, A. y Papademetris, X. A non-parametric vessel detection method for complex vascular structures. Medical Image Analysis, 13(1): 46-61, 2008.
26. Report of the Interregional meeting on Leishmaniasis among neighbouring endemic countries in the Eastern Mediterranean, African and European regions, Amman, Jordan, 23–25 September 2018. [cited 2019 Apr 22]; Available from: <https://www.who.int/leishmaniasis/resources/who-em-ctd-081-e/en/>
27. Manual of procedures for surveillance and control of Leishmaniasis in the Americas (in Spanish). [cited 2019 Apr 21]; Available from: <https://www.who.int/leishmaniasis/resources/978-92-75-32063-1/en/>
28. Essential leishmaniasis maps. [cited 2019 Apr 22]; Available from: https://www.who.int/leishmaniasis/leishmaniasis_maps/en/
29. Poostchi M, Silamut K, Maude RJ, Jaeger S, Thoma G. Image analysis and machine learning for detecting malaria. Transl Res; 194(2018):36–55. Available from: <https://doi.org/10.1016/j.trsl.2017.12.004>
30. Saeed MA, Jabbara A. "Smart diagnosis" of parasitic diseases by use of smartphones. J Clin Microbiol; [cited 2019 Apr 21];56(1):e01469-17. Available from: <http://www.ncbi.nlm.nih.gov/pubmed/29046408>
31. Coulibaly JT, Ouattara M, D'Ambrosio M V., Fletcher DA, Keiser J, Utzinger J, et al. Accuracy of Mobile Phone and Handheld Light Microscopy for the Diagnosis of Schistosomiasis and Intestinal Protozoa Infections in Côte d'Ivoire. Hsieh MH, editor. PLoS Negl Trop Dis; [cited 2019 Apr 21];10(6):e0004768. Available from: <https://dx.plos.org/10.1371/journal.pntd.0004768>
32. Dallet C, Kareem S, Kale I. Real time blood image processing application for malaria diagnosis using mobile phones. In: International Conference on Circuits and Systems. IEEE;2014. p. 2405–2408.
33. Rosado L, Da Costa JMC, Elias D, Cardoso JS. Automated Detection of Malaria Parasites on Thick Blood Smears via Mobile Devices. In: Procedia Computer Science [cited 2019 Apr 21].p.138–44. Available from: <https://www.sciencedirect.com/science/article/pii/S1877050916312029>
34. Farahi M, Rabbani H, Talebi A, Sarrafzadeh O, Ensafi S. Automatic segmentation of Leishmania parasite in microscopic images using a modified CV level set method. Seventh Int Conf Graph Image Process (ICGIP 2015). 2015;9817(January 2016):98170K.



www.revhipertension.com
www.revdiabetes.com
www.revsindrome.com
www.revistaavft.com